

Article

Electrodeposition of Copper/Carbonous Nanomaterial Composite Coatings for Heat-Dissipation Materials

Yasuki Goto ¹, Yota Kamebuchi ², Takeshi Hagio ^{1,3} , Yuki Kamimoto ³, Ryoichi Ichino ^{1,3,4,*} and Takeshi Bessho ⁵

¹ Department of Chemical Systems Engineering, Graduate School of Engineering, Nagoya University, Nagoya 464-8603, Japan; gotou.yasuki@e.mbox.nagoya-u.ac.jp (Y.G.); hagio@mirai.nagoya-u.ac.jp (T.H.)

² Department of Materials Science and Engineering, Graduate School of Engineering, Nagoya University, Nagoya 464-8603, Japan; kamerspksk@gmail.com

³ Green Mobility Research Institute, Institutes of Innovation for Future Society, Nagoya University, Nagoya 464-8603, Japan; kamimoto@gvm.nagoya-u.ac.jp

⁴ Institute of Materials and Systems for Sustainability, Nagoya University, Nagoya 464-8603, Japan

⁵ Toyota Motor Corporation, Toyota 471-8571, Japan; takeshi_bessho@mail.toyota.co.jp

* Correspondence: ichino.ryoichi@material.nagoya-u.ac.jp; Tel.: +81-52-747-3352

Received: 24 November 2017; Accepted: 19 December 2017; Published: 21 December 2017

Abstract: Carbonous nanomaterials are promising additives for composite coatings for heat-dissipation materials because of their excellent thermal conductivity. Here, copper/carbonous nanomaterial composite coatings were prepared using nanodiamond (ND) as the carbonous nanomaterial. The copper/ND composite coatings were electrically deposited onto copper substrates from a continuously stirred copper sulfate coating bath containing NDs. NDs were dispersed by ultrasonic treatment, and the initial bath pH was adjusted by adding sodium hydroxide solution or sulfuric acid solution before electrodeposition. The effects of various coating conditions—the initial ND concentration, initial bath pH, stirring speed, electrical current density, and the amount of electricity—on the ND content of the coatings were investigated. Furthermore, the surface of the NDs was modified by hydrothermal treatment to improve ND incorporation. A higher initial ND concentration and a higher stirring speed increased the ND content of the coatings, whereas a higher initial bath pH and a greater amount of electricity decreased it. The electrical current density showed a minimum ND content at approximately 5 A/dm². Hydrothermal treatment, which introduced carboxyl groups onto the ND surface, improved the ND content of the coatings. A copper/ND composite coating with a maximum of 3.85 wt % ND was obtained.

Keywords: copper; carbonous nanomaterial; composite coating; heat-dissipation material; nanodiamond

1. Introduction

Heat management has recently become a major issue in the electronics industry because of the continuous miniaturization of devices. This miniaturization has led to increased power densities; thus, effective heat removal is important to maintain and improve their performance [1–3]. Copper and its alloys have been widely used in the electronics industry as heat-dissipation materials because of its excellent thermal conductivity [3–5]. However, heat-dissipation materials with higher thermal conductivities are required for future electronics that will operate at much higher power densities.

Carbonous materials such as graphite, graphene, carbon nanofibers, carbon nanotubes, and diamonds are promising candidates for next-generation heat-dissipation materials because their thermal conductivity is 2 to 10 times greater than that of copper [3,5–10]. Various monolithic carbonous materials, including synthetic graphite sheets [6], graphite foams [8], a vertically aligned hybrid material of diamond thin platelets covered with a crystalline graphite layer [9], and highly oriented

pyrolytic graphite [10], have been reported to be good heat-dissipation materials. Although previous studies have demonstrated the effectiveness of carbonous materials as heat-dissipation materials, using them in a monolithic form is difficult because of their low formability and brittle nature [8,10].

Metal matrix composites using additives with high thermal conductivity are a possible solution to attain enhanced thermal conductivity [11,12]. Aluminum/silicon carbide particles composites are the key materials for thermal management at the present time [12,13], but their thermal conductivity, which reached 228 W/m·K when bimodal SiC particles were incorporated at a particle volume fraction of 0.74 [12], is still relatively low [14,15]. To further increase the thermal conductivity, additives with higher thermal conductivities are necessary. Meanwhile, composite coatings with carbonous nanomaterials incorporated into a metal matrix are receiving increasing attention for use in applications such as low-friction coatings [16,17], wear-resistant coatings [16–19], and corrosion-resistant coatings [16–20]. Embedding carbonous materials into a metal matrix can overcome some of the disadvantages associated with carbonous materials. Copper coatings for heat-dissipation applications are also expected to be improved through the incorporation of carbonous nanomaterials because of their excellent aforementioned thermal properties. Among the various carbonous nanomaterials, nanosized diamond—so-called nanodiamond (ND)—is the most promising additive for composite copper coatings because of its especially high and isotropic thermal conductivity [21]. Unlike most carbonous nanomaterials that exhibit anisotropic thermal conductivity, NDs do not require control of their orientation in composite coatings.

Composite coatings can be formed by electrolytic or electroless deposition from a coating bath containing additives, and the dispersibility of the additives is a key factor for achieving homogeneous and high additive incorporation [22,23]. To form copper/ND composite coatings, NDs should be highly dispersed in the coating bath and the ND size should be small to facilitate their effective incorporation [22–24]. Dispersants are often used to attain highly dispersed suspensions in composite coatings [23–25]; however, the thermal conductivity of the composite coating is deteriorated through the inclusion of the dispersants [25]. A different strategy is thus necessary to improve the dispersibility of NDs. Surface modification is a prospective approach to improve the dispersibility of carbonous nanomaterials [26–28], and hydrothermal treatment in strong inorganic acids is known to enable the surface modification of carbonous nanomaterials [28–30].

Even though copper/ND composite coatings are expected to be prospective heat-dissipation materials, the effects of the electrodeposition coating conditions and the surface modification of ND are not well known. In the present study, copper/ND composite coatings were prepared by electrodeposition and the effect of various coating conditions (i.e., the initial ND concentration, initial bath pH, stirring speed, electrical current density, and the amount of electricity) on the ND content of the coating was investigated. Furthermore, the surface modification of ND by hydrothermal treatment was carried out to improve ND incorporation into the coatings.

2. Materials and Methods

2.1. Materials

Copper sulfate pentahydrate ($\text{CuSO}_4 \cdot 5\text{H}_2\text{O}$, purity $\geq 99.5\%$, Nacalai Tesque, Inc., Kyoto, Japan), nitric acid (HNO_3 , conc. 60%–62%, Nacalai Tesque, Inc.), concentrated sulfuric acid (H_2SO_4 , conc. $\geq 95\%$, Nacalai Tesque, Inc.), and sodium hydroxide (NaOH , purity $\geq 97\%$, Nacalai Tesque, Inc.) were used as received. Purified detonation NDs were acquired from NOF Corporation (Tokyo, Japan). The NDs were well crystallized diamonds forming agglomerates composed of primary particles approximately 5 to 10 nm in diameter, as shown in Figure 1. Surface-modified NDs were prepared by the hydrothermal treatment of NDs in concentrated H_2SO_4 solutions. H_2SO_4 was selected to avoid contamination by other anions. ND (0.15 g) was suspended in 5 mL of concentrated H_2SO_4 in a Teflon container, which was subsequently sealed in a stainless-steel jacket for hydrothermal treatment at 493 K for 2 h.

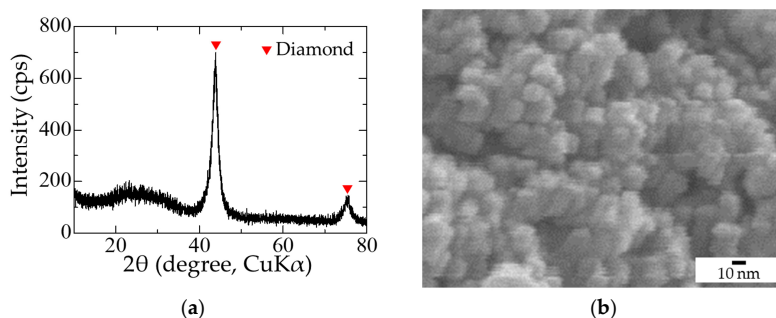


Figure 1. Characterization of initial nanodiamonds (NDs): (a) X-ray diffraction; (b) scanning electron microscope.

2.2. Preparation of Copper/ND Composite Coatings

Copper substrates (B-60 hull cell cathode plates, Yamamoto-MS Co., Ltd., Tokyo, Japan) were masked, leaving an area of 400 mm² (20 mm × 20 mm) for electrodeposition. The copper substrates were washed with diluted HNO₃ solution for 10 s and completely dried after being rinsed with distilled water. The copper substrates, a platinum wire, and an Ag/AgCl electrode in a saturated KCl solution were used as the cathode, anode, and reference electrode, respectively. A 0.1 M or 1 M CuSO₄ bath was prepared by dissolving CuSO₄·5H₂O in distilled water. Then, 0, 0.15, 0.25, 0.5, 1.0, or 1.5 g of ND was added to the CuSO₄ bath of 50 mL. When non-treated NDs were used, the pH of the bath was adjusted using a solution of NaOH or H₂SO₄. By contrast, when surface-modified NDs were used, the NDs were added along with the 5 mL of concentrated H₂SO₄ solution used for hydrothermal treatment; however, the total bath volume was maintained at 50 mL, and no further pH adjustment was carried out. The NDs were then ultrasonically suspended for 1 h using an ultrasonic homogenizer (VC-505, 20 kHz, 200 W, Sonics and Materials, Inc., Newtown, CT, USA) to disperse the NDs. The temperature of the suspension was maintained near room temperature by using a glass tempering beaker (T 250, KGW-Isotherm GmbH, Karlsruhe, Germany) with tap water continuously flowing through it.

Electrodeposition was performed at room temperature using a galvanostat (HZ-5000, Hokuto Denko Corp., Tokyo, Japan), and the stirring speed, current density, and amount of electricity were varied. The effects of the initial ND concentration, initial pH, stirring speed, current density, amount of electricity, and the surface modification of the NDs were investigated. The experimental conditions are shown in Table 1. Five to ten replicate experiments were performed for the first set of experimental conditions (Exp. No. 1) to confirm the uncertainties of the data. For the rest, two to four runs were performed under each set of investigated conditions. Their average values were adopted; however, for experimental conditions that overlapped between sets, average values of the total runs were used. The standard error of each data set is indicated as error bars in the figures.

Table 1. Coating conditions used in this study.

Exp. No.	Initial CuSO ₄ Concentration (M)	Initial ND Concentration (g/L)	Initial pH	Stirring Speed (rpm)	Current Density (A/dm ²)	Amount of Electricity (C)	Surface Modification of ND
1	0.1	0–30	2	500	1	20	–
2	1	3	0–4	500	0.1	20	–
3	0.1	3	2	250–750	1	20	–
4	1	20	2	500	1–25	20	–
5	0.1	3	2	500	1	10–100	–
6	0.1	3	2 or ≤ 0 ¹	500	1 or 10	20	None or HT ²

Notes: ¹ Below detection limit; ² HT: Hydrothermal treatment at 493 K for 2 h in concentrated H₂SO₄ solution.

2.3. Characterization of Copper/ND Composite Coatings

The ND content of the coatings was evaluated via a combustion method using a carbon–sulfur simultaneous analysis device (EMIA-510, Horiba, Ltd., Kyoto, Japan). The coating was fired at 1623 K along with the copper substrate under an oxygen atmosphere, and the generated gas was measured by infrared absorption. The concentrations of the composite components were calculated using the following equations:

$$V_t = \frac{m_C}{M_t} \times 100 = \frac{V_c M_c + V_s M_s}{M_t} \approx \frac{V_c M_c}{M_t} (\because V_s \approx 0) \quad (1)$$

$$V_c = V_t \times \frac{M_t}{M_c} \quad (2)$$

where V_t , V_c , and V_s are the carbon contents of the test piece (wt %), coating (wt %), and the substrate (wt %), respectively; M_t , M_c , and M_s are the mass of the test piece (g), coating (g), and the substrate (g), respectively; and m_C is the overall carbon mass in the test piece (g). The measurement error was considered to be less than ± 0.1 wt % from the results from standard samples and pure copper coatings.

The microstructure of the coatings was observed using a scanning electron microscope (SEM, JSM-6330F, JEOL Ltd., Tokyo, Japan) operating at 15 kV. The effect of the hydrothermal treatment on the NDs was evaluated on the basis of the functional groups on the surface of the NDs via Fourier-transform infrared spectroscopy (FTIR, Spectrum 100s, PerkinElmer, Inc., Waltham, MA, USA).

3. Results and Discussion

The effect of initial ND concentration, initial pH, stirring speed, current density, amount of electricity, and surface modification of NDs is discussed on the basis of the results of each of the experiments detailed in Table 1.

3.1. Effect of Initial ND Concentration of the Coating Bath

The effect of the initial ND concentration on the ND content of the final coating is shown in Figure 2. The ND content in the coating increases with increasing the initial ND concentration in the bath and finally reaches a plateau value of 0.8 wt % at approximately 10 g/L under this set of experimental conditions. The greater incorporation of NDs with increasing initial ND content is explained as follows. When the initial ND concentration increases, more NDs are transported to the surface of the copper substrate; thus, more NDs can be incorporated. However, at higher ND concentrations, where the surface becomes nearly covered with NDs, the NDs remaining in the bath can no longer approach the substrate surface easily because it is covered with NDs. The interactions or collisions of NDs in the bath with the NDs on the surface of the substrate reach an equilibrium condition and prevent a further increase in the amount of incorporated NDs. An initial concentration of 10 g/L appears to correspond to the concentration where complete surface coverage by NDs is achieved. Similar trends have been reported for composite coatings in various systems such as a copper–multiwalled carbon nanotube system [25] and a nickel–aluminum nitride system [31]. The larger standard error at initial ND concentrations above 20 g/L may be due to the aggregation of NDs.

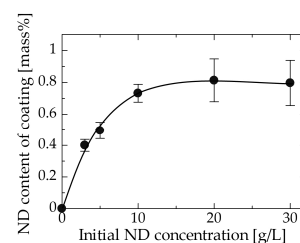


Figure 2. Relation between the initial ND concentration in the bath and the ND content of the coating.

3.2. Effect of Initial pH of the Coating Bath

The effect of initial pH on the ND content of the coating is shown in Figure 3. The range of pH in this experiment was decided to be 0 to 4 because copper hydroxide formed in the coating bath when the pH was increased to values greater than 4. Figure 3 shows that more ND particles were incorporated at lower pH values, especially when the pH was less than 2. The drastic increase in ND content in the coating below pH 2 may be caused by several factors. One factor is the effect of surface functional groups on the ND. ND is known to have various functional groups on its surface [26]. Conceivably, excess protons (H^+) may cover the ND surface when an acidic solution contacts these functional groups on the ND surface, imparting the ND with a positive charge, which promotes its movement toward the cathode side. Another possibility is the effect of zeta potential. The zeta potential of detonation NDs without surface modification has been reported to be positive at low pH levels [27]. A positive zeta potential would also promote the movement of NDs to the cathode side.

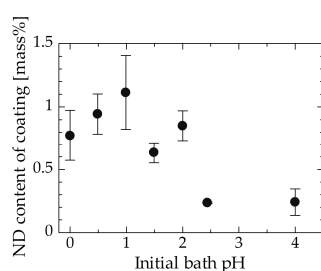


Figure 3. Relation between the initial pH of the bath and the ND content of the coating.

3.3. Effect of the Stirring Speed of the Coating Bath

Figure 4 shows the relation between the stirring speed and the ND content of the coating at a fixed bath ND concentration of 3 g/L. The ND content in the coating increased with increasing the stirring speed in the range investigated in this experiment (Exp. No. 3, Table 1). This behavior is attributed to the increase in frequency of NDs approaching the substrate. When the stirring speed is low, the concentration of NDs near the coating surface might decrease after deposition begins as a consequence of the adsorption rate of ND onto the substrate surface being higher than the feed rate. In addition, insufficient convection would cause incomplete dispersion of the NDs and may further lead to aggregation of the NDs. Incomplete dispersion or aggregation might decrease the number of NDs transferred to the cathode by gravity settling, thereby lowering the final ND content of the coating.

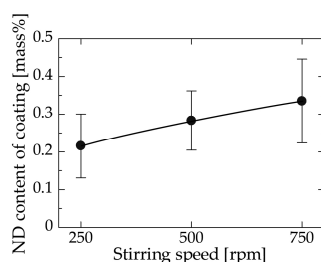


Figure 4. Relation between the stirring speed and the ND content of the coating.

3.4. Effect of the Current Density during Electrodeposition

The effect of the current density during electrodeposition on the ND content of the coating is shown in Figure 5. Current density can be interpreted as the deposition rate. The ND content decreased with increasing the current density, reached a minimum of approximately 0.23 wt % at 5 A/dm², and then increased thereafter. The existence of a minimum value may indicate a change in the dominant mechanism. The following mechanism is proposed. In general, the particle content in

composite coatings is determined by the competition between the deposition rate of the metal matrix and the adsorption rate of the additive particles. In the range from 1 to 5 A/dm², the adsorption of NDs onto the substrate surface may have become dominant, resulting in an increase in the ND content of the coating at especially low current densities. A similar behavior has been observed in composite coatings that follow Guglielmi's model [32]. By contrast, when the current density is greater than 5 A/dm², the adsorption of NDs must have been promoted by the high overpotential resulting from the increase in the current density [33], thereby enhancing the incorporation of NDs into the coating. In addition, the high current density may have promoted copper deposition bridging the incorporated NDs, leading to better adhesion. Molina et al. [34] found that nickel bridging alumina particles deposited when a high voltage was applied in the electrodeposition of nickel on aluminum alloy/alumina particles composite, while nickel could not be deposited on the surface of alumina particles at low voltages. A similar phenomenon may have occurred at high current densities.

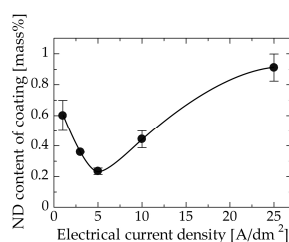


Figure 5. Relation between the current density and the ND content of the coating.

3.5. Effect of the Amount of Electricity Used for Electrodeposition

Figure 6 shows the relation between the amount of electricity and the ND content of the coating. The amount of electricity nearly corresponds to the thickness of the coating. Coatings deposited using relatively small amounts of electricity, i.e., the thinner coatings, contained more ND particles compared with those deposited using larger amounts of electricity, i.e., thicker coatings. These results suggest that NDs were incorporated during the early step of electrodeposition and were unevenly distributed in the thickness direction. This may be because NDs poorly adsorb onto substrates that exhibit substantial roughness due to their difficulty in entering the dents. SEM observation of the surface was conducted to investigate the change of the surface morphology of the coating when the amount of electricity was varied. As evident in the surface SEM images (Figure 7a–d), the grain size of the deposited copper matrix was small when the amount of electricity was small and increased with increasing the amount of electricity. The surface roughness seemed to increase as grains became larger. The ND adsorption onto the coating surface was hindered by the increase in surface roughness corresponding to the increase in the amount of electricity. Such a change in the surface morphology of the coating may be responsible for the decrease in the ND content of the coating. In addition, a certain thickness, i.e., amount of electricity, may have been necessary for the copper to cover the initially adsorbed NDs since the copper must have deposited mainly on the copper matrix and not on the ND surface, as discussed in Section 3.4 [34]. This may have hindered further NDs from being incorporated into the copper matrix in the experimental condition considered in this study.

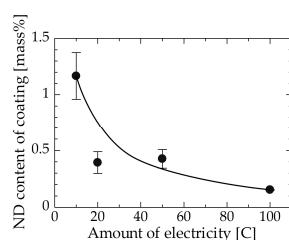


Figure 6. Relation between the amount of electricity and the ND content of the coating.

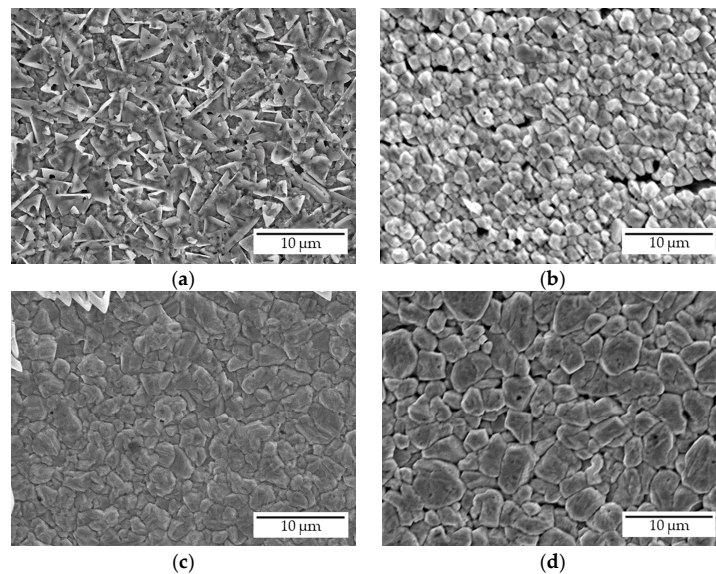


Figure 7. Surface SEM images of composite coatings deposited at an amount of electricity of (a) 10 C, (b) 20 C, (c) 50 C, and (d) 100 C.

3.6. Effect of the Surface Modification of NDs

3.6.1. Characterization of Surface-Modified NDs

Surface modification of NDs was carried out by hydrothermal treatment at 493 K for 2 h in concentrated H_2SO_4 solution. The surface-modified NDs were characterized using FTIR measurements because acid treatment has been reported to introduce functional groups onto the surface of NDs. The obtained FTIR spectra are shown in Figure 8. NDs that were only immersed in H_2SO_4 were also characterized for comparison. The peak near 1600 cm^{-1} indicates a decrease in the number of $\text{C}=\text{C}$ bonds, and the peak at approximately 1700 cm^{-1} indicates an increase in the abundance of $\text{C}=\text{O}$ bonds. In Figure 8c, a peak from approximately 3500 cm^{-1} to approximately 2500 cm^{-1} is also observed. This peak may indicate an increase in the number of $-\text{OH}$ bonds derived from the carboxyl groups. These results show that the numbers of $-\text{OH}$ bonds and $-\text{C}=\text{O}$ bonds increased on the surface of the ND particles as a result of the hydrothermal treatment, whereas the number of $\text{C}-\text{C}$ bonds decreased. Consequently, the results suggest that carboxyl groups were introduced onto the NDs as a result of the hydrothermal treatment [35]. Jiang et al. reported that the oxidation treatment of activated carbon using concentrated H_2SO_4 at 533 K introduced mainly carboxyl groups (COO^- species) and hydroxyl groups ($-\text{OH}$) [36]. A similar phenomenon may have occurred in the present study.

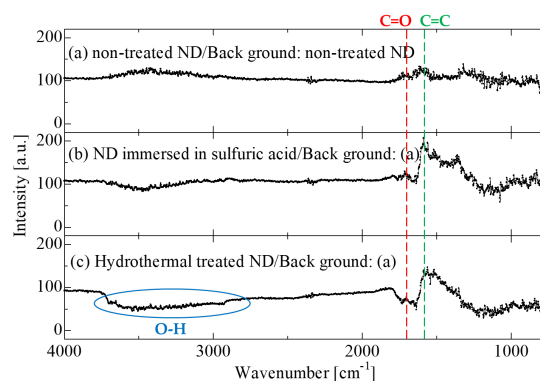


Figure 8. Peak obtained from FTIR measurements.

3.6.2. Effect of Surface Modification on the ND Content of Coatings

The ND content of coatings deposited using surface-modified NDs are summarized in Figure 9. The ND content of the coating increased by 30 to 60% when surface-modified NDs were used. Hydrothermal treatment has been reported to improve the colloidal stability of the ND particles in water [37], which likely led to our observed increase in the amount of NDs incorporated. Moreover, the positive charge induced by the excess protons, as discussed in Section 3.2, may have been intensified by the additional carboxyl groups introduced by the hydrothermal treatment. Using the hydrothermally treated ND particles under conditions of a 0.1 M CuSO₄ bath, an initial ND concentration of 3 g/L, a stirring speed of 500 rpm, a current density of 10 A/dm², and an amount of electricity of 20 C, a coating with an ND content as high as 3.85 mass % ND, corresponding to nearly 10 vol % ND, was attained.

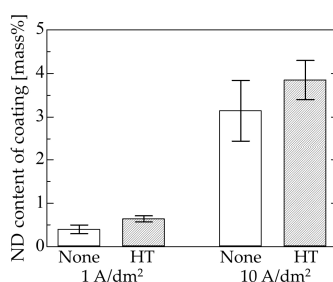


Figure 9. Effect of hydrothermal treatment on the ND content of the coating.

4. Conclusions

In this study, copper/ND composite coatings were prepared by electrodeposition and the effects of various coating conditions, initial ND concentration, initial bath pH, stirring speed, electrical current density, and the amount of electricity on the ND content of the coatings were investigated. Furthermore, surface modification of the ND by hydrothermal treatment was performed to improve ND incorporation. A higher initial ND concentration and a higher stirring speed increased the ND content of the coatings, whereas a higher initial bath pH and a greater amount of electricity decreased it. The electrical current density showed a minimum ND content at approximately 5 A/dm². Hydrothermal treatment, which introduced carboxyl groups onto the ND surface, improved the ND content of the coatings. A copper/ND composite coating with a maximum of 3.85 mass % ND was obtained. The results indicate that the ND content of the coatings increased when the NDs approached the substrate at a high frequency, and that NDs are unevenly distributed in the thickness direction of the coatings.

Acknowledgments: We express our profound gratitude to NOF Corporation for providing the ND particles.

Author Contributions: Yota Kamebuchi mainly performed the experiments and analyses; Yasuki Goto and Takeshi Hagio considered the data and wrote the paper; Yuki Kamimoto and Ryoichi Ichino conceived and designed the experiments; Takeshi Bessho performed part of the analyses and gave important advice throughout the experiments.

Conflicts of Interest: The authors declare no conflict of interest.

References

1. Anandan, S.S.; Ramalingam, V. Thermal management of electronics: A review of literature. *Therm. Sci.* **2008**, *12*, 5–26. [[CrossRef](#)]
2. Li, J.; Li, X.; Fan, C.; Yao, H.; Chen, X.; Liu, Y. Study on the preparation of a high-efficiency carbon fiber dissipating coating. *Coatings* **2017**, *7*, 94. [[CrossRef](#)]
3. Silvain, J.F.; Veillère, A.; Lu, Y. Copper-carbon and aluminum-carbon composites fabricated by powder metallurgy processes. *J. Phys. Conf. Ser.* **2014**, *525*, 012015. [[CrossRef](#)]

4. Koráb, J.; Štefánik, P.; Kavecký, Š.; Šebo, P.; Korb, G. Thermal conductivity of unidirectional copper matrix carbon fibre composites. *Compos. Part A* **2002**, *33*, 577–581. [[CrossRef](#)]
5. Jiang, B.; Wang, H.; Wen, G.; Wang, E.; Fang, X.; Liu, G.; Zhou, W. Copper–graphite–copper sandwich: Superior heat spreader with excellent heat-dissipation ability and good weldability. *RSC Adv.* **2016**, *6*, 25128–25136. [[CrossRef](#)]
6. Ngo, Q.; Cruden, B.A.; Cassell, A.M.; Sims, G.; Meyyappan, M.; Li, J.; Yang, C.Y. Thermal interface properties of Cu-filled vertically aligned carbon nanofiber arrays. *Nano Lett.* **2004**, *4*, 2403–2407. [[CrossRef](#)]
7. Balandin, A.A. Thermal properties of graphene, carbon nanotubes and nanostructured carbon materials. *Nat. Mater.* **2011**, *10*, 569–581. [[CrossRef](#)] [[PubMed](#)]
8. Lin, W.; Yuan, J.; Sundén, B. Review on graphite foam as thermal material for heat exchangers. In Proceedings of the World Renewable Energy Congress 2011-Sweden, Energy End-Use Efficiency Issues (EEE), Linköping, Sweden, 8–13 May 2011; pp. 748–755.
9. Santos, N.F.; Holz, T.; Santos, T.; Fernandes, A.J.S.; Vasconcelos, T.L.; Gouvea, C.P.; Archanjo, B.S.; Achete, C.A.; Silva, R.F.; Costa, F.M. Heat dissipation interfaces based on vertically aligned diamond/graphite nanoplatelets. *ACS Appl. Mater. Interfaces* **2015**, *7*, 24772–24777. [[CrossRef](#)] [[PubMed](#)]
10. Wang, Q.; Han, X.H.; Sommers, A.; Park, Y.; Joen, C.T.; Jacobi, A. A review on application of carbonaceous materials and carbon matrix composites for heat exchangers and heat sinks. *Int. J. Refrig.* **2012**, *35*, 7–26. [[CrossRef](#)]
11. Arpon, R.; Molina, M.J.; Saravanan, A.R.; Garcia-Cordovilla, C.; Louis, E.; Narciso, J. Thermal expansion behaviour of aluminium/SiC composites with bimodal particle distributions. *Acta Mater.* **2003**, *51*, 3145–3156. [[CrossRef](#)]
12. Molina, M.J.; Narciso, J.; Weber, L.; Mortensen, A.; Louis, E. Thermal conductivity of Al–SiC composites with monomodal and bimodal particle size distribution. *Mater. Sci. Eng. A* **2008**, *480*, 483–488. [[CrossRef](#)]
13. Molina, M.J.; Prieto, R.; Narciso, J.; Louis, E. The effect of porosity on the thermal conductivity of Al–12 wt % Si/SiC composites. *Scr. Mater.* **2009**, *60*, 582–585. [[CrossRef](#)]
14. Qu, X.H.; Zhang, L.; Wu, M.; Ren, S.B. Review of metal matrix composites with high thermal conductivity for thermal management applications. *Prog. Nat. Sci. Mater. Int.* **2011**, *21*, 189–197. [[CrossRef](#)]
15. Prieto, R.; Molina, M.J.; Narciso, J.; Louis, E. Fabrication and properties of graphite flakes/metal composites for thermal management applications. *Scr. Mater.* **2008**, *59*, 11–14. [[CrossRef](#)]
16. Wang, L.; Gao, Y.; Xue, Q.; Liu, H.; Xu, T. Effects of nano-diamond particles on the structure and tribological property of Ni-matrix nanocomposite coatings. *Mater. Sci. Eng. A* **2005**, *390*, 313–318. [[CrossRef](#)]
17. Burkat, G.K.; Fujimura, T.; Dolmatov, V.Y.; Orlova, E.A.; Veretennikova, M.V. Preparation of composite electrochemical nickel–diamond and iron–diamond coatings in the presence of detonation synthesis nanodiamonds. *Diam. Relat. Mater.* **2005**, *14*, 1761–1764. [[CrossRef](#)]
18. Medelienė, V.; Stankevič, V.; Grigucevičienė, A.; Selskienė, A.; Bikulčiu, G. The study of corrosion and wear resistance of copper composite coatings with inclusions of carbon nanomaterials in the copper metal matrix. *Mater. Sci.* **2011**, *17*, 132–139. [[CrossRef](#)]
19. Shakoor, A.R.; Waware, S.U.; Ali, K.; Kahraman, R.; Popelka, A.; Yusuf, M.M.; Hasan, A. Novel electrodeposited Ni-B/Y₂O₃ composite coatings with improved properties. *Coatings* **2017**, *7*, 161. [[CrossRef](#)]
20. Praveen, B.M.; Venkatesha, T.V. Generation and corrosion behavior of Zn-Nano sized carbon black composite coating. *Int. J. Electrochem. Sci.* **2009**, *4*, 258–266.
21. Pumera, M. Nanocarbon electrochemistry. In *Electrochemistry. Volume 11, Nanosystems Electrochemistry*; Wadhawan, J.D., Compton, R.G., Eds.; Royal Society of Chemistry: London, UK, 2012; pp. 104–123.
22. Kuo, S.L.; Chen, Y.C.; Ger, M.D.; Hwu, W.H. Nano-particles dispersion effect on Ni/Al₂O₃ composite coatings. *Mater. Chem. Phys.* **2004**, *86*, 5–10. [[CrossRef](#)]
23. Güler, E.S. Effects of electroplating characteristics on the coating properties. In *Electrodeposition of Composite Materials*; Mohamed, A.M.A., Golden, T.D., Eds.; InTech: Rijeka, Croatia, 2016; pp. 27–37. ISBN 978-953-51-2270-8.
24. Shrestha, N.K.; Saji, T. Composite plating using an electro-active surfactant—A new approach to incorporate high amount of ceramic particles into a metal matrix. *J. Surf. Finish. Soc. Jpn.* **2006**, *57*, 489–496. [[CrossRef](#)]
25. Arai, S.; Saito, T.; Endo, M. Cu–MWCNT composite films fabricated by electrodeposition. *J. Electrochem. Soc.* **2010**, *157*, D147–D153. [[CrossRef](#)]

26. Gibson, N.; Shenderova, O.; Luo, T.J.M.; Moseenkov, S.; Bondar, V.; Puzyr, A.; Purtov, K.; Fitzgerald, Z.; Brenner, D.W. Colloidal stability of modified nanodiamond particles. *Diam. Relat. Mater.* **2009**, *18*, 620–626. [[CrossRef](#)]
27. Xu, X.; Yu, Z.; Zhu, Y.; Wang, B. Influence of surface modification adopting thermal treatments on dispersion of detonation nanodiamond. *J. Solid State Chem.* **2005**, *178*, 688–693. [[CrossRef](#)]
28. Kharissova, O.V.; Kharisov, B.I.; Ortiz, E.G.C. Dispersion of carbon nanotubes in water and non-aqueous solvents. *RSC Adv.* **2013**, *3*, 24812–24852. [[CrossRef](#)]
29. Moraes, R.A.; Matos, C.F.; Castro, E.G.; Schreiner, W.H.; Oliveira, M.M.; Zarbin, A.J.G. The effect of different chemical treatments on the structure and stability of aqueous dispersion of iron- and iron oxide-filled multi-walled carbon nanotubes. *J. Braz. Chem. Soc.* **2011**, *22*, 2191–2201. [[CrossRef](#)]
30. Cheng, J.; He, J.; Li, C.; Yang, Y. Facile approach to functionalize nanodiamond particles with V-shaped polymer brushes. *Chem. Mater.* **2008**, *20*, 4224–4230. [[CrossRef](#)]
31. Aal, A.A.; Bahgat, M.; Radwan, M. Nanostructured Ni–AlN composite coatings. *Surf. Coat. Technol.* **2006**, *201*, 2910–2918. [[CrossRef](#)]
32. Bahrololoom, M.E.; Sani, R. The influence of pulse plating parameters on the hardness and wear resistance of nickel–alumina composite coatings. *Surf. Coat. Technol.* **2005**, *192*, 154–163. [[CrossRef](#)]
33. Guo, D.; Zhang, M.; Jin, Z.; Kang, R. Pulse plating of copper–ZrB₂ composite coatings. *J. Mater. Sci. Technol.* **2006**, *22*, 514–518.
34. Molina, J.M.; Saravanan, R.A.; Narciso, J.; Louis, E. Surface modification of 2014 aluminium alloy–Al₂O₃ particles composites by nickel electrochemical deposition. *Mater. Sci. Eng. A* **2004**, *383*, 299–306. [[CrossRef](#)]
35. Krueger, A.; Lang, D. Functionality is key: Recent progress in the surface modification of nanodiamond. *Adv. Funct. Mater.* **2012**, *22*, 890–906. [[CrossRef](#)]
36. Jiang, Z.; Liu, Y.; Sun, X.; Tian, F.; Sun, F.; Liang, C.; You, W.; Han, C.; Li, C. Activated carbons chemically modified by concentrated H₂SO₄ for the adsorption of the pollutants from wastewater and the dibenzothiophene from fuel oils. *Langmuir* **2003**, *19*, 731–736. [[CrossRef](#)]
37. Matsubara, H. Fabrication of novel materials by the incorporation of nanodiamond into plated films. *J. Surf. Sci. Soc. Jpn.* **2009**, *30*, 279–286. [[CrossRef](#)]



© 2017 by the authors. Licensee MDPI, Basel, Switzerland. This article is an open access article distributed under the terms and conditions of the Creative Commons Attribution (CC BY) license (<http://creativecommons.org/licenses/by/4.0/>).